Chapter 5
Density Gradient Ultracentrifugation of Colloidal Nanostructures

Liang Luo, Qixian Xie and Yinglan Liu

Abstract According to the centrifugation theory, various factors, such as the media density (ρ_m), radius (r) and thickness (h) of nanostructures, and solvation shell thickness (t) in different media, will directly influence the particle behavior during the density gradient centrifugation process. Density gradient centrifugation has become a promising tool to purify nanomaterials, such as metal nanostructures, carbon materials (carbon nanotubes and graphene), non-metal nanostructures (e.g., rare-earth nanostructures and oxide nanostructures). For the practical separation, as demonstrated in previous chapters, on the basis of the theoretical analysis of the target nanostructures and the preliminary separation, one can optimize the centrifugation according to the comprehensive consideration. While after all, the optimization direction of nanoseparation should be mainly focused on the net density of nanostructures and media. In this chapter, we will discuss the separation examples according to the dimensional difference of colloidal nanostructures, including 0D, 1D, 2D nanostructures, and assemblies/clusters.

Keywords Zero dimensional · One dimensional · Two dimensional Assemblies · Clusters

5.1 Separation of Zero-Dimensional Nanostructures

Quantitatively, a theoretical assay would be important for optimizing separation of zero-dimensional materials, and the kinetic equation of zero-dimensional nanostructures can be demonstrated as:

$$\frac{d^2x}{dt^2} + \frac{9\eta}{2\rho_p(r+h)^2}\frac{dx}{dt} + \frac{\rho_m - \rho_p}{\rho_p}\omega^2 x = 0 \tag{5.1}$$

Zero-dimensional nanostructures with different size and shape could be separated with different rates. For the nanostructures with net density much higher than the media density ($\rho_p > \rho_m$), such as noble metal, they can usually be separated by rate-zonal separation with high efficiency. While if the net density of nanostructures

X. Sun et al., *Nanoseparation Using Density Gradient Ultracentrifugation*, SpringerBriefs in Molecular Science, https://doi.org/10.1007/978-981-10-5190-6_5

(ρ_p) is relative small or the density difference of fractions is very small, they would be separated by using isopycnic separation. Furthermore, the net density difference of nanostructures can be enlarged based on some strategies, such as changing the solvation shell thickness (t) by introducing surfactant, or increasing media viscosity by introducing polymers.

The separation of nanoparticles with high net density is usually simple. By using the aqueous multiphase systems (MuPSs) as media for rate-zonal centrifugation, Akbulut et al. [2] separated the gold nanoparticles from the nanorods with different sizes and shapes successfully (Fig. 5.1b). Similarly, Osman M. Bakr et al. [3] also used rate-zonal density gradient centrifugation method to separate diamond nanocrystals with diameters mainly <10 nm. While as the size decreases (lower than 5 nm), the net density is much smaller, and the density difference is also dramatically decreased due to the existence of solvation shell (see Eq. 4.20 in Chap. 4). Hence, for the separation of ~4 nm FeCo@C nanoparticles, Sun et al. [1] encapsulated the nanoparticles with polyethylene glycol (PEG), and enlarged the hydration shell thickness, namely, enlarged the density difference of nanoparticles. With the iodixanol/water solutions (20 + 30 + 40 + 60%) as density gradient media and rate-zonal separation method, FeCo@C nanocrystallines with coated PEG in average size were efficiently separated from 1.5 to 5.6 nm with monodispersity, exhibiting the fine enough degree of density gradient separation (Fig. 5.1a).

Though powerful, aqueous separation of nanoparticles has several limitations: 1. It is only suitable for the aqueous soluble nanoparticles, while a lot of nanoparticles

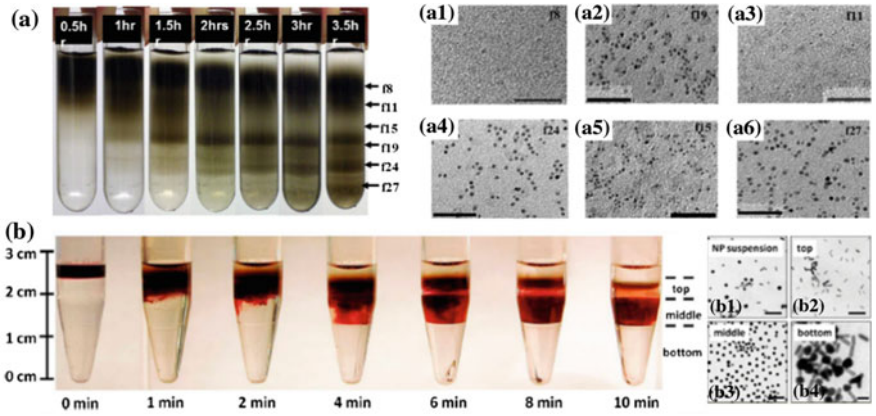

Fig. 5.1 **a** Optical and TEM images showing the separation of 4 nm FeCo@C nanoparticles (Digital camera images of ultracentrifuge tubes taken at 30 min intervals). (a1–a6) TEM images of different fractions labeled in (**a**). Scale bars: 50 nm; **b** the evolution of the penetration of nanoparticles into an aqueous three-phase system. The solvent of the suspension of nanoparticles (i.e., water) stayed as a clarified layer on top of the system, small nanorods (i.e., the desired product) penetrated slightly into the top phase, small nanospheres migrated to the middle phase, and large particles of both shapes sedimented to the bottom. (b1–b4) TEM images of suspension of nanoparticles (suspension of NP) and samples collected from the layers as shown in (**b**). The scale bar in each image corresponds to 200 nm

were synthesized in organic phase and got solubilized therein (such as Au, CdSe, and Si nanocrystals), and phase transfer might cause serious aggregation. 2. A large mass ratio of salts or solutes are added inside to make the gradient, which significantly complicated the consequent purification procedure to obtain separated nanoparticles. Such separation requirement promotes the emergence of organic phase separation. Therein the gradient media are organic phase (polar or non-polar) to avoid the aggregation of dispersed colloidal nanoparticles, and keep them isolated. Besides, after sampling the product out, the organic media can be vaporized to get "pure" sample. Since unbounded surfactants or soluble by-products could be isolated from the colloidal products, the rate-zonal separation method can also be used for purification of nanocrystals in organic phase.

Additionally, the nanomaterials prepared in organic phase would inevitably aggregate in aqueous solution and should be separated with organic gradient media. Besides, after sampling the product, the residual organic media can be easily removed by various treatments, such as evaporation. Similarly, the simple, rapid, and effective density gradient centrifugation method can also be used for separation and purification of nanocrystals in organic phase. Through dispersing the colloidal nanoparticles in nonhydroxylic solvents using ultracentrifugation in an organic density gradient which gives rapid separation and concomitant purification, Sun's group [4] separated the Au colloidal nanoparticles synthesized in oleylamine. The thin layer (usually 0.1–0.4 mL) of the Au colloidal suspension was placed on a density gradient made by mixing different ratios of cyclohexane and tetrachloromethane (50–90% of CCl_4 by volume; density range, 1.13–1.41 g/cm3). With the centrifugation speed of 50000 rpm ($\sim$330000 g), the Au colloidal particles were finely separated as monodispersed 4.8, 7.2, 8.0, 9.3, and 10.9 nm, and the size of the error range was less than 1.5 nm (Fig. 5.2a). In addition, to make the separation more visible, fluorescent CdSe NPs (CdSe concentration: $\sim$25 mg/mL) were synthesized and separated by using the cyclohexane/tetrachloromethane gradient (Fig. 5.2b).

For the small density of zero-dimensional nanoparticles, if the size is up to several hundred nanometers, such as silica nanoparticles, the rate-zonal centrifugation can be simply used. Chen et al. [5] separated various silica particles with size from 280 nm up to 440 nm successfully in $\sim$1 min by centrifugation. The polydispersity index improved largely, e.g., from 0.116, 0.084, 0.071, and 0.102 to 0.013, 0.007, 0.006, and 0.009 for 80 nm, 260 nm, 740 nm, and 5 lm silica particles, respectively (Fig. 5.3).

While for the very small sized and narrow distributed silicon nanocrystalline, one can change the solvation shell thickness to enlarge the apparent density. Geoffrey A. Ozin et al. [6] modified the silicon nanocrystalline with decylsilane to increase the hydration shell thickness and realized the size separation of the silicon nanocrystalline (Fig. 5.4) by using the 40 wt% 2,4,6-tribromotoluene in chlorobenzene as the density gradient medium. They further investigated the size-dependent structural, optical, electrical, and biological properties of silicon.

This method enables nanoparticles separated in miscible organic solvents. Since a large number of metal and semiconductor colloidal NPs are synthesized in organic

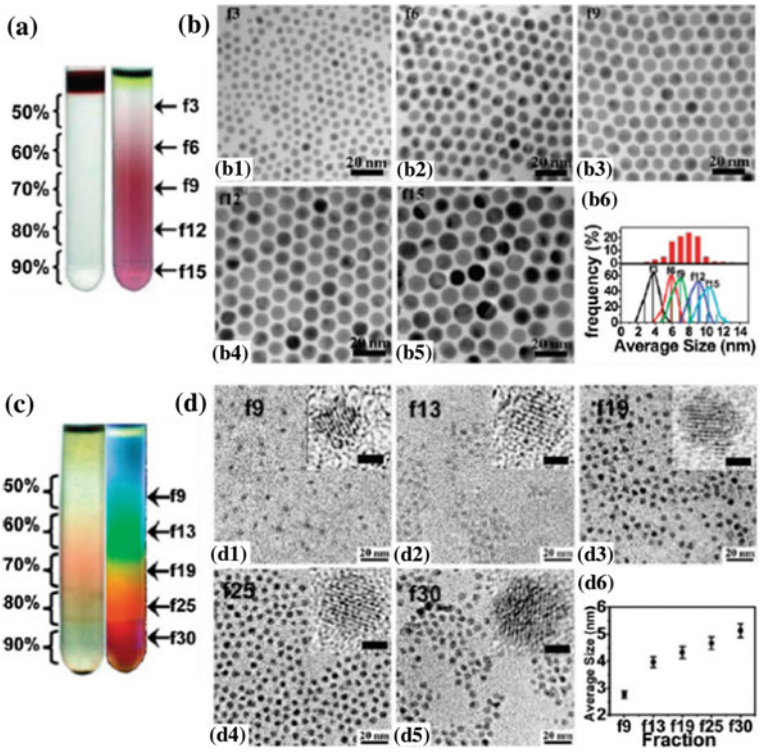

Fig. 5.2 **a** Digital images of ultracentrifuge vessels containing Au nanoparticles before (left vessel) and after (right vessel) separation at 25000 rpm for 12 min. **b** TEM images of typical fractions. The graph in the bottom right corner shows a comparison of the size distribution difference before (red columns in the upper section) and after (colored columns in the lower section) centrifugation separation. Each size histograms was measured from at least 200 particles. **c** Digital camera images of ultracentrifuge vessels containing CdSe nanoparticles using a cyclohexane + tetrachloromethane gradient after separation at 50000 rpm for 60 min. The left image was recorded under white light; the right image was recorded under UV irradiation at 365 nm. **d** HRTEM images of typical CdSe nanoparticle fractions. Magnified individual nanoparticles are shown in the insets (the bars in the insets are 2 nm). The graph in the bottom right corner shows the size evolution of particles along the centrifuge vessel

systems, the separation, purification, and transformation can be employed directly on the raw product mixture by density gradient separation method.

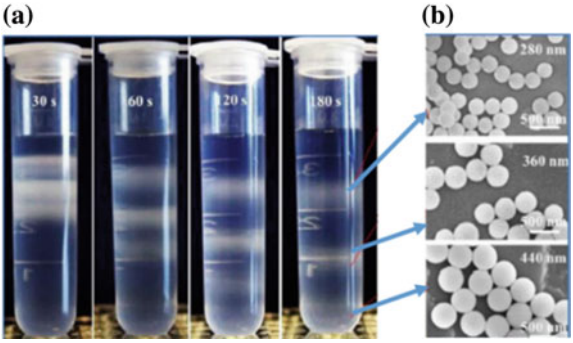

Fig. 5.3 **a** Centrifugal separation of 280, 360, and 440 nm silica particles, through a gradient of 400, 500, 600, 700, and 800 mg/mL sucrose layered from top to bottom at 25 °C, 600 g, and centrifugal time of 30, 60, 120, and 180 s, respectively. **b** The SEM results illustrate the size and shape

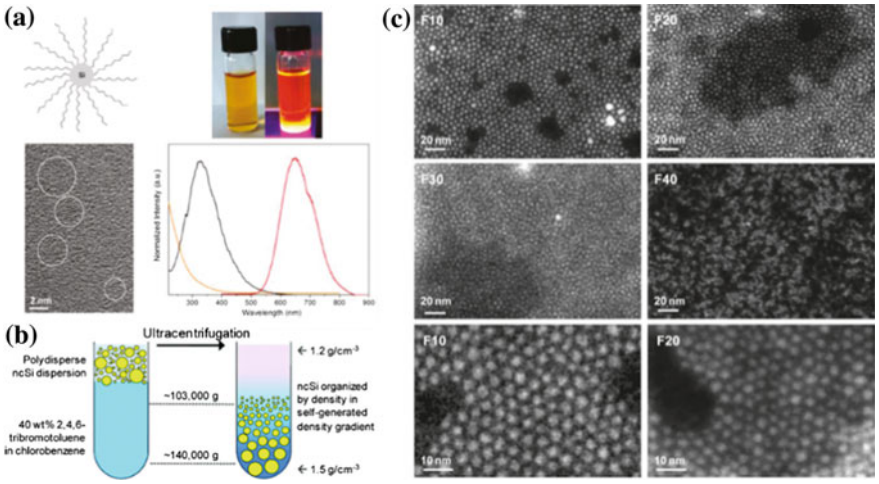

Fig. 5.4 **a** Decyl-capped silicon nanocrystals; **b** the schematic diagram of the ultracentrifugation process; **c** Size analysis of monodisperse ncSi fractions

5.2 Separation of One-Dimensional Nanostructures

For the separation of one-dimensional nanostructures, the density gradient ultracentrifugation rate separation (DGURS) method has also usually emerged as an efficient tool for the separation. The kinetic equation of one-dimensional nanostructures can be simplified as:

$$\frac{d^2x}{dt^2} + \left[\frac{3}{2}(r+h)^2(l+2h)\right]^{-\frac{2}{3}} \frac{9\eta\theta}{2\rho_p}\frac{dx}{dt} + \frac{\rho_m - \rho_p}{\rho_p}\omega^2 x = 0 \tag{5.2}$$

Similarly, the rate-zonal centrifugation can be simply used for the separation of nanorods with large density (ρ_p). For example, after synthesizing CdS nanorods by solvothermal method with the amine as the solvent, Sun et al. [7] used a five-layer density gradient (30%, 40%, 50%, 60%, and 70% cyclohexane/CCl4 solutions) and centrifugation at 30 000 rpm (relative centrifugal force, RCF = 113600 g) for 70 min. The NRs in the fractions in the bottom half of the tube showed a significant increase in diameter (from ~4.2 nm to ~6.5 nm) while only a relatively small decrease in length (from ~12.3 nm to ~10.6 nm). They successfully sorted CdS NRs according to different aspect ratio, and the separated fractions showed significant size-dependent fluorescence property (Fig. 5.5).

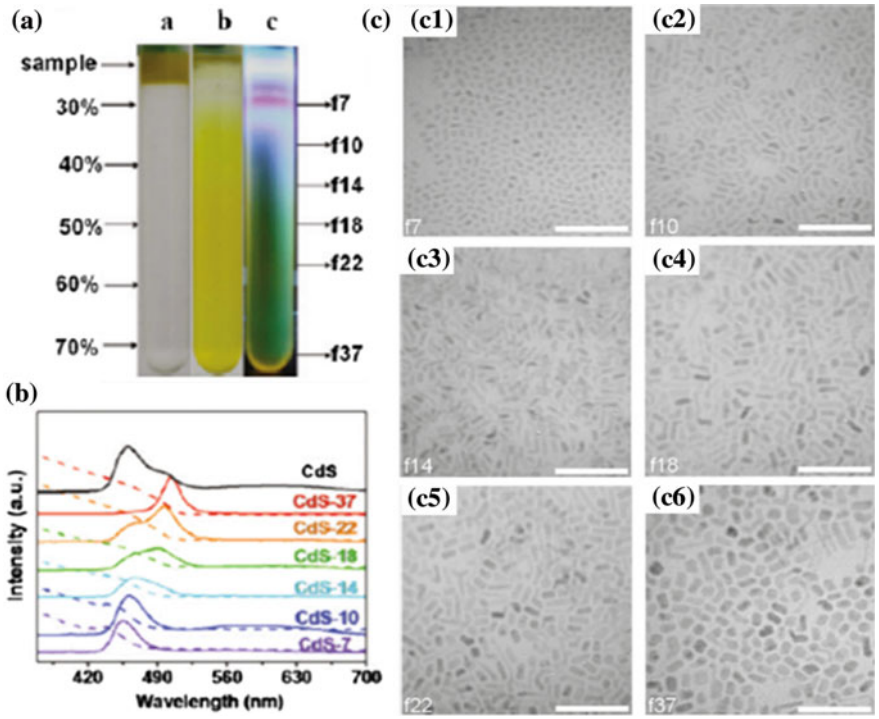

Fig. 5.5 Digital camera images of the ultracentrifuge tubes before and after separation at 30 000 rpm: **a** before separation; after centrifugation for 70 min; separated NRs under 365 nm UV irradiation (fX means the Xth fraction going from top to bottom); **b** Photoluminescence (solid lines) and absorbance spectra (dotted lines) of typical fractions after separation (the black line shows the photoluminescence spectrum of the CdS product before separation); (c1–c6)TEM images of CdS NR fractions separated by DGURS (the scale bar is 50 nm in each case)

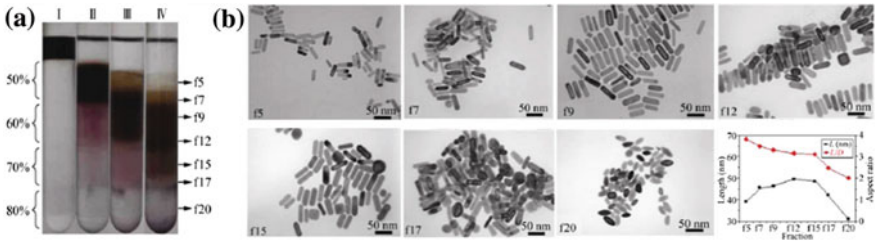

Fig. 5.6 **a** Digital camera images of the ultracentrifuge tubes before and after separation at 10,000 r/min: (I) before separation; (II) after separation for 10 min; (III) after separation for 20 min; (IV) after separation for 30 min; **b** TEM images of separated Au NRs in typical fractions. The graph in the bottom right corner shows the evolution of the lengths (squares) and aspect ratios (triangles) in the Au NRs in different fractions

Besides, by using different mixing ratios of EG with aqueous CTAB solution (50%–80% of EG by volume), and centrifugation speed with 10,000 r/min (17,000 g) for 10 min, Liu et al. [8] separated the gold nanorods with different length, namely aspect ratios. Au NRs were separated into distinct zones along the centrifuge tube (Fig. 5.6). He et al. [9] also successfully applied density gradient centrifugation method to achieve the separation of gold nanorods (Fig. 5.7).

As for the separation of one-dimensional nanostructures with high density, such as Au nanorods, the sedimentation rate is usually high in ultracentrifugal field. If the target one-dimensional nanostructures are with very similar length, according to the kinetic equation, one can also adjust the viscosity of gradient media to decrease the sedimentation rate and realize efficient separation. By adding the poly (2-ethyl-2-oxazoline), Liu et al. [10] increased the viscosity, changed the sedimentation behaviors of Au nanorods, and successfully separated the Au–NRs with size ranging from 25.6 to 26.1 nm through 5500 g within 5 min, which appears to be the fastest method for separation of Au–NRs (Fig. 5.8).

Different with metal nanostructures, the carbon nanotubes possess extreme small density and diameter ($\sim$0.7–1.1 nm), particularly, the density difference is very small, which remained a big challenge for the effective separation of them. As a breakthrough, Hersam's group [11] first introduced the DGC method to sort carbon nanotubes. Combing with the method of enriching DNA to wrapped semiconducting SWNTs (single-walled carbon nanotubes), they increased the hydration shell thickness and enlarged the density difference. It is worth noting that, even after modification of DNA, the density difference of SWNTs is still very small (1.11–1.17 g cm^{-3}), and SWNTs can be separated by isopycnic mode, with different colored bands. This finding could likely be applied to separate other nanostructures in which external functionalization or relative hydration of the surfaces varies with size (Fig. 5.9).

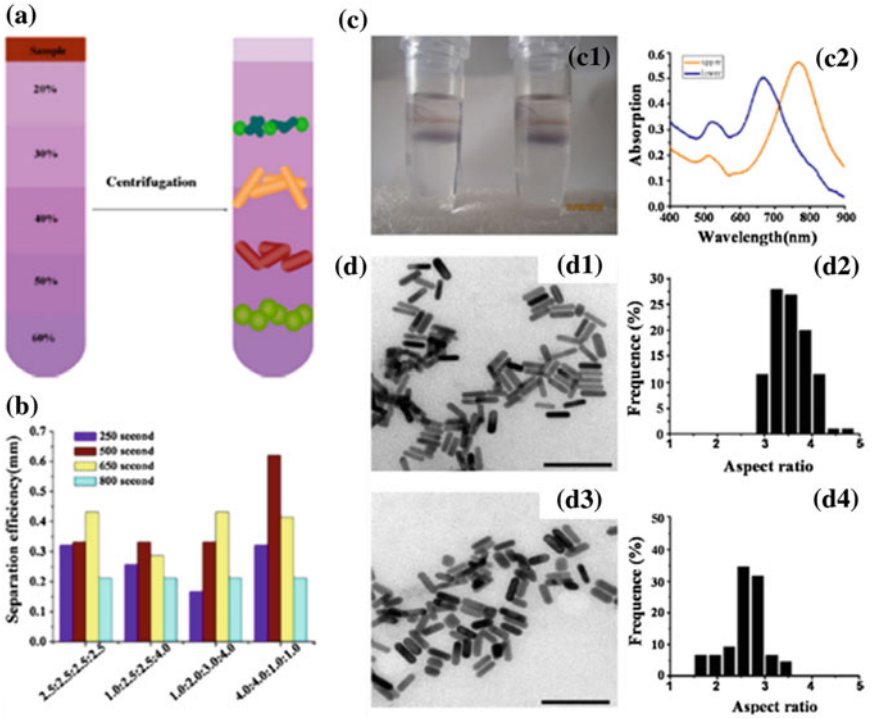

Fig. 5.7 **a** Predicated separation profile of a complicated sample containing rods with diverse aspect ratios and spheres with different diameters. **b** Calculated separation efficiency of two equal-mass gold nanorods of aspect ratios 2 and 4, respectively, during sucrose gradient centrifugation using different sucrose layer thickness and centrifugal time. **c** Optical image of the centrifuge tube and the UV–visible spectra of the two layers after separation. **d** TEM image and aspect ratio distribution of nanorods from the upper layer, and the lower layer. All particles and rods with aspect ratio less than 1.5 were not counted and did not show up in the histogram data (The scale bar is 100 nm)

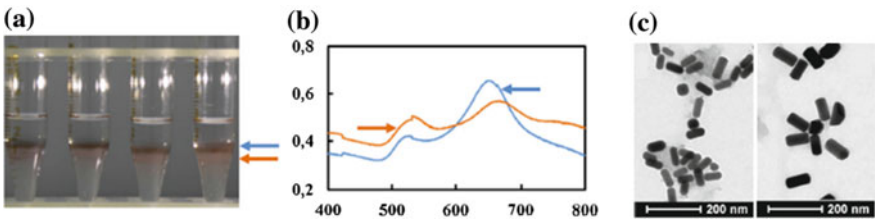

Fig. 5.8 **a** Pictures of the centrifuge tubes taken at the end of four parallel runs; **b** Normalized UV–VIS spectra of the gold nanorods in the different fractions; **c** TEM images of the gold nanorods in the top and the bottom fractions

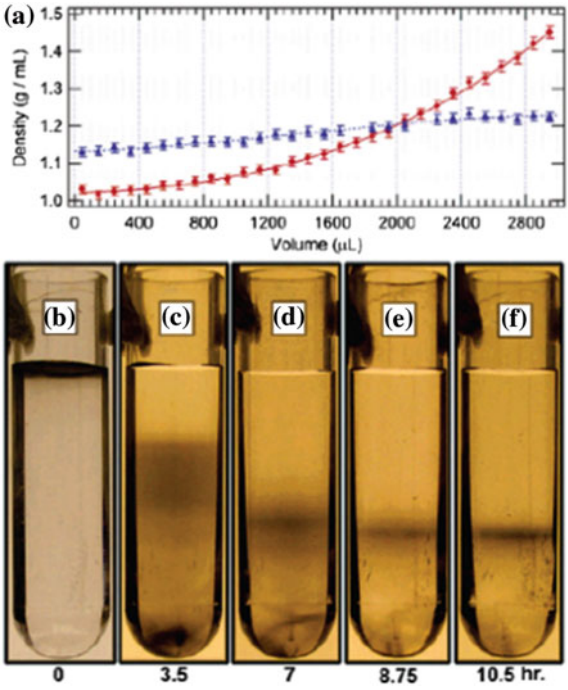

Fig. 5.9 Redistribution of iodixanol and SWNTs during ultracentrifugation. **a** Profile of the density gradient before (dotted line) and after (solid line) centrifugation. During centrifugation, the iodixanol redistributed. **b–f** Sedimentation of SWNTs in a density gradient before and after 3.5, 7, 8.75, and 10.5 h of ultracentrifugation

Based on the finding of the isopycnic mode applied on the separation of nanotubes, Green et al. [12] used sodium cholate (SC) and sodium dodecyl sulfate (SDS) rather than DNA which is relatively more prohibitive and cheap to modify the carbon nanotubes, and the purity of the single-walled carbon nanotubes after separation could reach 99% (Fig. 5.10a). Later, Hersam's group [13] used three bile salts (sodium cholate (SC), sodium dodecyl sulfate (SDS), and sodium dodecylbenzene sulfonate (SDBS)) to modify the carbon nanotubes. By the scalable technique of density gradient ultracentrifugation, they isolated narrow distributions of SWNTs in which >97% and within a 0.02nm diameter range (Fig. 5.10b).

Hersam's group [14] has also shown that density gradient ultracentrifugation could be used to separate double-wall nanotubes (DWNTs) from mixtures of single- and multi-wall nanotubes through differences in their density, which could be used in transparent conductors. They added approximately 70% DWNTs into 110 mL of 1 wt% SC aqueous solution, with a loading of $\sim$2 mg/mL in a steel beaker. Then the CNTs were efficiently sorted from polydispersed mixtures to monodispersed SWNTs with different diameters and DWNTs (Fig. 5.11).

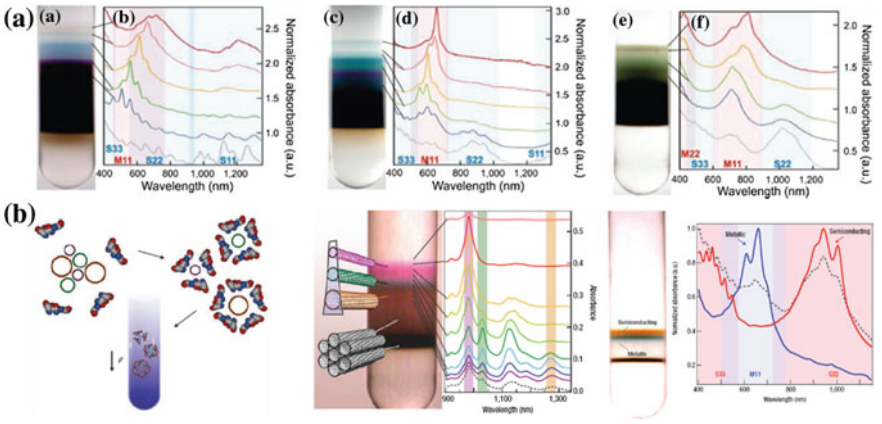

Fig. 5.10 **a** Photographs of ultracentrifuge tubes following DGU, Sorted SWNTs (solid) were collected from gradients at points labeled; **b** Sorting of SWNTs by diameter, bandgap and electronic type using density gradient ultracentrifugation. Schematic of surfactant encapsulation and sorting, where r is density, and Photographs and optical absorbance (1 cm path length) spectra after separation using density gradient ultracentrifugation; Photograph of laser-ablation-grown SWNTs separated

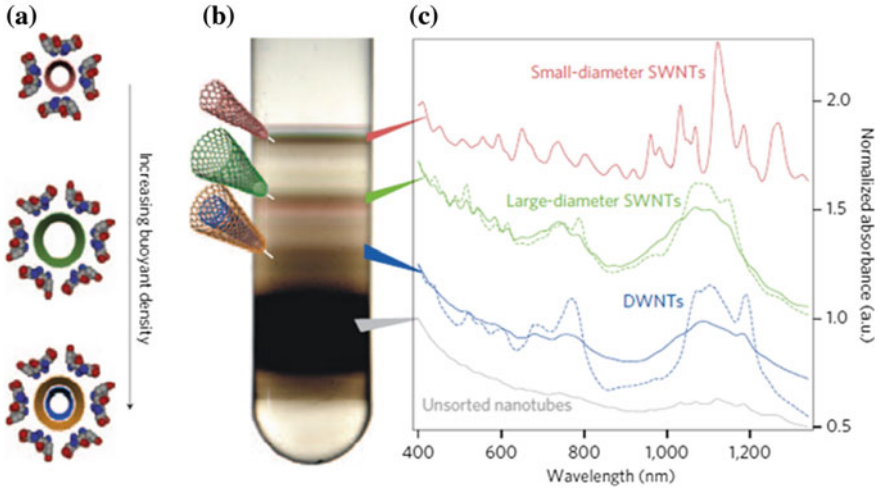

Fig. 5.11 Separation of carbon nanotubes by number of walls using density differentiation. **a** Schematic illustration of carbon nanotube encapsulation by sodium cholate and its effect on nanotube buoyant density. **b** Photograph of a centrifuge tube following the first-iteration density gradient ultracentrifugation (DGU) separation of as-received nanotubes. **c** Optical absorbance spectra of the bands of material taken from the centrifuge tube at the locations indicated

5.3 Separation of Two-Dimensional Nanostructures

Recent years, more and more attentions have been attracted to the 2D materials, such as graphene. The separation of the two-dimensional nanomaterials referred kinetic equation can be simplified as:

$$\frac{d^2x}{dt^2} + \left[\frac{3}{2}(r+h)^2(l+2h)\right]^{-\frac{2}{3}} \frac{9\eta\theta}{2\rho_p}\frac{dx}{dt} + \frac{\rho_m - \rho_p}{\rho_p}\omega^2 x = 0 \tag{5.3}$$

Graphene, as the most widely investigated two-dimensional material, the thickness (r) is very small, inducing the very little density difference for different layered graphene samples. Similarly to the separation of carbon nanotubes, surface modification is an effective choice to increase the hydration shell thickness (t) and enlarge the density difference, and thereby improve the separation efficiency. Sun's group [15, 16] separated the graphene oxide (GO) solution by rate-zonal separation method. Through the typical centrifugation conditions were 5 min at 50,000 rpm ($\sim$300 kg, SW65 Rotor, Beckman Coulter); they finally obtained GO fractions in accordance with the size difference which is found to be related to the oxidation degree (Fig. 5.12b). By studying the properties of separated fractions, it is found that small nanosheets possess weak visible region absorption, strong fluorescence, and high oxidation degree.

The density gradient centrifugation could also be used for the separation of other kinds of two-dimensional materials besides graphene, such as layered double

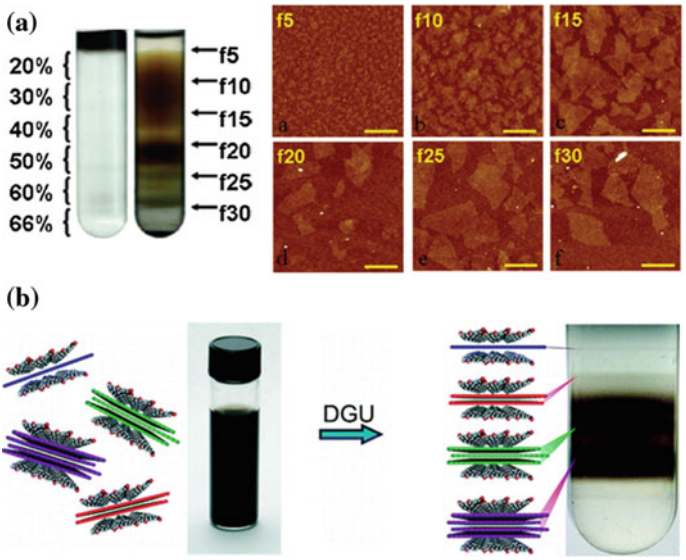

Fig. 5.12 **a** Schematic illustration of the graphene exfoliation process. Graphite flakes are combined with sodium cholate (SC) in aqueous solution; **b** Digital camera images of the ultracentrifuge tubes after separation at 50 K rpm, Tapping-mode AFM images (2 × 2 μm^2, scale bar: 500 nm) of different fractions of CRG as labeled in left tube

hydroxides and zeolite. Michael Tsapatsis et al. [17] used density gradient centrifugation to purify the zeolite product, through rate-zonal centrifugation of nanosheets in a multilayered density gradient; they separated exfoliated nanosheets from larger unexfoliated particles. The MFI-nanosheets were centrifuged (Beckman Coulter, Avanti J-20 XP equipped with JA25.50 rotor) in four 50 mL FEP centrifuge tubes at 40,000 g for 3 h to sediment zeolite nanosheets at the bottom of the centrifuge tubes. This application example indicated that a nonlinear density gradient of organic solvents could be used to purify exfoliated MFI-nanosheets prepared by melt compounding of multilamellar MFI.

While for the separation of graphene nanosheets with similar size and different layers, even with surface modifications, the density difference is usually still very limited, which requires extremely fine separation. As a breakthrough, Hersam et al. [18] used two-plane amphiphilic surfactant (sodium deoxycholate) to stabilize the package of graphene sheets, and the different thicked fractions can be sorted with controlled thickness by isopycnic separation. During this process, the aqueous solution phase approach is enabled by the planar amphiphilic surfactant sodium cholate (SC), which forms a stable encapsulation layer on each side of the suspended graphene sheets (Fig. 5.12a).

Similarly, by adding cesium chloride (CsCl) to iodixanol, increasing its maximum buoyant density to the point, Hersam et al. [19] sorted the high-density two-dimensional nanomaterial rhenium disulfide (ReS_2) with isopycnic density

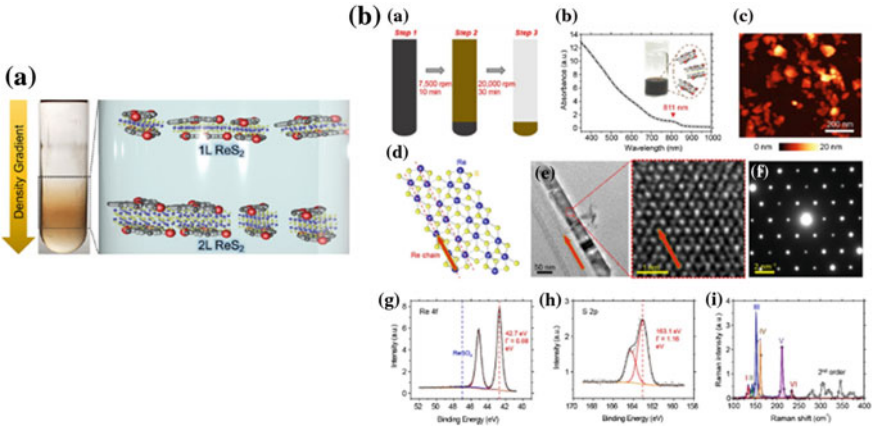

Fig. 5.13 **A** Schematic illustration of the ReS_2 separated process; **B a** Experimental procedure to enrich few-layer ReS_2 nanosheets. **b** Optical absorbance spectrum of the resulting ReS_2 aqueous dispersion with a peak at 811 nm. Inset: photograph of the as-prepared ReS_2 dispersion with the schematic illustrating ReS_2 nanosheets surrounded by SC. **c** Atomic force microscopy image of solution-processed ReS_2 following deposition on a Si wafer. **d** A schematic of the atomic structure of ReS_2 (blue: Re atom; yellow: S atom; red dotted line: Re chain direction). **e** A transmission electron microscopy image of a ReS_2 nanosheet and a high-resolution TEM image. The red arrow indicates the direction of a Re chain. **f** Selected area electron diffraction pattern of a ReS2 nanosheet. **g**, **h** X-ray photoelectron spectroscopy data for the (**g**) Re 4f and **h** S 2p core levels. **i** Raman spectrum of ReS_2 nanosheets

gradient ultracentrifugation. After resulting dispersion was centrifuged at 7500 rpm to remove unexfoliated ReS_2 powder, the ReS_2 nanosheets with relatively large lateral sizes were ultracentrifuged at 20 000 rpm to collect (Fig. 5.13). The density gradient ultracentrifugation separation technique has been widely used for the separation of different sizes and dimensions. Even though there is some difference of viscous resistance for different morphologied nanostructures, the apparent density of nanostructures with surface solvation shell is usually the key factor.

5.4 Separation of Assemblies/Clusters

Nanomaterial assemblies have good application prospects in many fields. Compared with monomers, the density of assemblies/cluster is related to the assemble degree and can be considered as different sized single nanoparticles. From a separate point of view, the assemblies/cluster can also be effectively separated. Examples will be given to verify the centrifugation theory (Fig. 5.14).

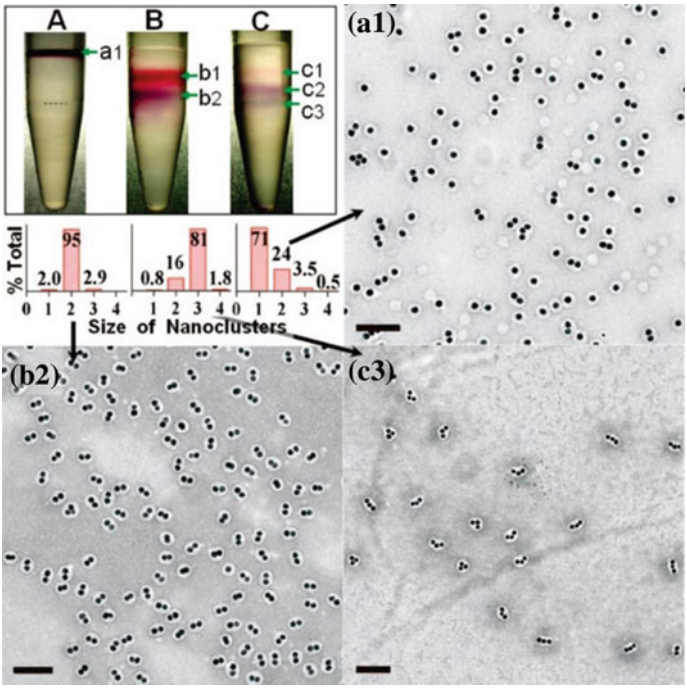

Fig. 5.14 **a** A typical setup of differential centrifugation, where 62% and 11% aq. CsCl and then AuNPn@PSPAA in water were layered from bottom to top. **b** The result of A after 20 min centrifugation. **c** Separation result of a pre-enriched trimer sample. (a1, b2, and c3) TEM images of the respective fractions indicated in **a**–**c** (see large-area views in the Supporting Information); the histograms are shown in the insets. Scale bars: 100 nm

Chen et al. [20, 21] encapsulated gold nanoparticles with amphiphilic diblock copolymers (PSPAA) to form core-shell nanoassemblies. Based on rate-zonal separation, AuNP dimers, and trimers were separated with excellent purity. Since structural intactness is critical for the construction of any nanoassembly, the approach offers a facile separation method without additional inconvenience. Their subsequent research revealed that the structural uniformity of the "hot spots" therein reduced the ambiguities in calculating and interpreting the respective SERS enhancement factors, and the relative intensity ratios of the nanoclusters ($I_{2NP} = 16I_{1NP}$ and $87I_{3NP}$) involve few assumptions and are thus more reliable (Figs. 5.15 and 5.16).

Carbon nanodots (CDs) have gained research relevance as novel carbon nanomaterials. Due to their extremely high colloidal stability, common ultracentrifugation has failed in sorting them. Luo et al. [22] introduce an ultracentrifugation method using a hydrophilicity gradient to sort such non-sedimental CDs. CDs were pre-treated by acetone to form clusters. Such clusters "de-clustered" as they were forced to sediment through media comprising gradients of ethanol and water with varied volume ratios. During the centrifugation, primary CDs with varied sizes and degrees of carbonization detached from the clusters to become well dispersed in the corresponding gradient layers. Their settling level was highly dependent on the varied hydrophilicity and solubility of the environmental media.

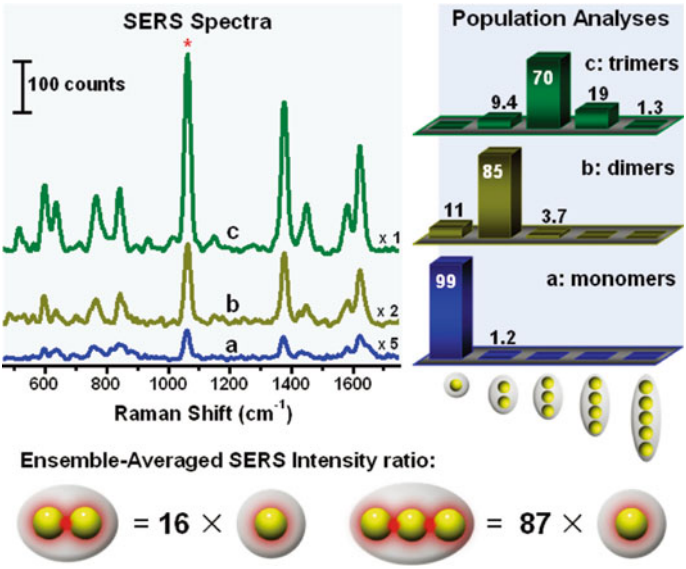

Fig. 5.15 SERS spectra of the samples enriched with **a** monomers, **b** dimers, and **c** trimers of Au@Ag NPs (**d**) 20 nm; excitation: 785 nm at 290 mW; insets: the histograms of these samples). The schematics in the lower panel show the SERS intensity ratio of the nanoclusters

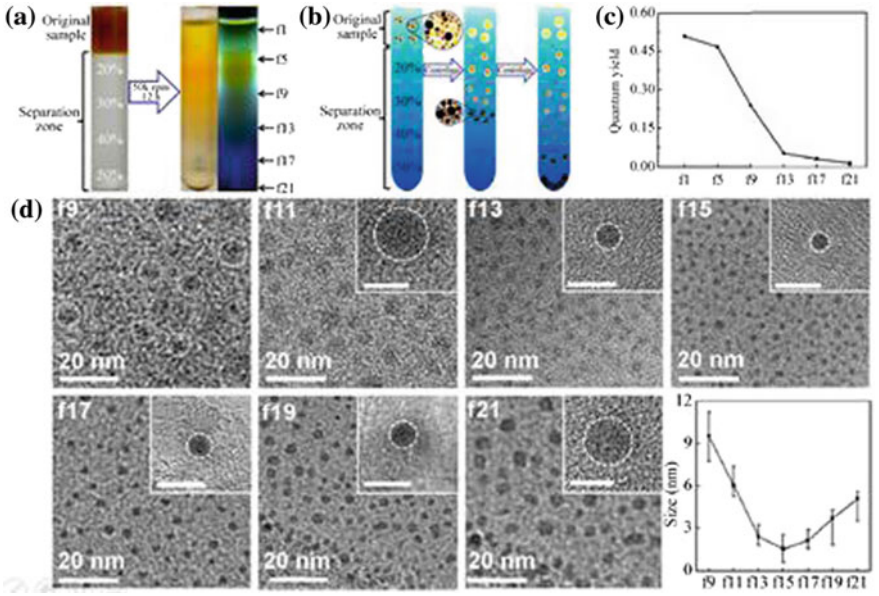

Fig. 5.16 **a** Digital photographs of the centrifuge tube (under ambient light) before and (left: under ambient light, and right: under UV light) after centrifugation. **b** Scheme of proposed mechanism of separation: CDs were clustered at starting point and de-clustered at successive layers with increasing water content during sedimentation. **c** QY variation of typical fractions, showing that more stable CDs have higher fluorescence

References

1. Sun X, Tabakman SM, Seo WS et al (2009) Separation of nanoparticles in a density gradient: FeCo@C and gold nanocrystals. Angew Chem Int Edit 48 (5):939–942
2. Akbulut O, Mace CR, Martinez RV et al (2012) Separation of nanoparticles in aqueous multiphase systems through centrifugation. Nano Lett 12(8):4060–4064
3. Peng W, Mahfouz R, Pan J et al (2013) Gram-scale fractionation of nanodiamonds by density gradient ultracentrifugation. Nanoscale 5(11):5017–5026
4. Bai L, Ma X, Liu J et al (2010) Rapid separation and purification of nanoparticles in organic density gradients. J Am Chem Soc 132(7):2333–2337
5. Hu C, Chen Y (2015) Uniformization of silica particles by theory directed rate-zonal centrifugation to build high quality photonic crystals. Chem Eng J 271:128–134
6. Mastronardi ML, Hennrich F, Henderson EJ et al (2011) Preparation of monodisperse silicon nanocrystals using density gradient ultracentrifugation. J Am Chem Soc 133(31):11928–11931
7. Ma X, Kuang Y, Bai L et al (2011) Experimental and mathematical modeling studies of the separation of zinc blende and wurtzite phases of CdS nanorods by density gradient ultracentrifugation. ACS Nano 5(4):3242–3249
8. Li S, Chang Z, Liu J et al (2011) Separation of gold nanorods using density gradient ultracentrifugation. Nano Res 4(8):723–728
9. Xiong B, Cheng J, Qiao Y et al (2011) Separation of nanorods by density gradient centrifugation. J Chromatogr A 1218(25):3823–3829

10. Dong S, Wang Y, Tu Y et al (2016) Separation of gold nanorods by viscosity gradient centrifugation. Microchim Acta 183(3):1269–1273
11. Arnold MS, Stupp SI, Hersam MC (2005) Enrichment of single-walled carbon nanotubes by diameter in density gradients. Nano Lett 5(4):713–718
12. Green AA, Hersam MC (2008) Colored semitransparent conductive coatings consisting of monodisperse metallic single-walled carbon nanotubes. Nano Lett 8(5):1417–1422
13. Arnold MS, Green AA, Hulvat JF et al (2006) Sorting carbon nanotubes by electronic structure using density differentiation. Nat Nanotechnol 1(1):60–65
14. Green AA, Hersam MC (2009) Processing and properties of highly enriched double-wall carbon nanotubes. Nat Nanotechnol 4(1):64–70
15. Green AA, Hersam MC (2009) Solution phase production of graphene with controlled thickness via density differentiation. Nano Lett 9(12):4031–4036
16. Sun X, Liu Z, Welsher K et al (2008) Nano-graphene oxide for cellular imaging and drug delivery. Nano Res 1(3):203–212
17. Sun X, Luo D, Liu J et al (2010) Monodisperse chemically modified graphene obtained by density gradient ultracentrifugal rate separation. ACS Nano 4(6):3381–3389
18. Agrawal KV, Topuz B, Jiang Z et al (2013) Solution-processable exfoliated zeolite nanosheets purified by density gradient centrifugation. AIChE J 59(9):3458–3467
19. Kang J, Sangwan VK, Wood JD et al (2016) Layer-by-layer sorting of rhenium disulfide via high-density isopycnic density gradient ultracentrifugation. Nano Lett 16(11):7216–7223. https://doi.org/10.1021/acs.nanolett.6b03584
20. Chen G, Wang Y, Tan LH et al (2009) High-purity separation of gold nanoparticle dimers and trimers. J Am Chem Soc 131(12):4218–4219
21. Chen G, Wang Y, Yang M et al (2010) Measuring ensemble-averaged surface-enhanced raman scattering in the hotspots of colloidal nanoparticle dimers and trimers. J Am Chem Soc 132(11):3644–3645
22. Deng L, Wang X, Kuang Y et al (2015) Development of hydrophilicity gradient ultracentrifugation method for photoluminescence investigation of separated non-sedimental carbon dots. Nano Res 8(9):2810–2821